 / ISSN (Print): 2446-9246 / ISSN (Online): 2446-9432

Simulation Software for the ISDB-T_B Modulation System

Cristiano Akamine and Yuzo Iano

***Abstract*—This paper presents a simulation tool for the ISDB-T_B modulator, to perform complex analyses in each processing stage. From a Broadcast Transport Stream (BTS) file you can follow the processing performed in each modulator block to the final transmission stage. It is possible to make real transmissions with the RF files generated in the simulator with the use of a vector signal generator. A mathematical and practical approach to the operation of each modulator block is performed starting with the description of the BTS signal up to the final transmission stage.**

***Index Terms*—Broadcast Transport Stream – Orthogonal Frequency Division Multiplexing (BST-OFDM), Integrated Digital Broadcasting System – Terrestrial (ISDB-T), Modulator, Simulation.**

I. Introduction

THE Integrated Services Digital Broadcasting - Terrestrial (ISDB-T) modulation system [1] is designed to operate with various types of services occupying a TV channel with a bandwidth of 6, 7 or 8 MHz. The system is very flexible and allows the combination of multiple services, such as portable reception, mobile, and fixed with unequal protection errors on the same channel. The system uses the Band Segmented Transmission - Orthogonal Frequency Division Multiplexing (BST-OFDM) modulation in which each segment uses a wide band corresponding to 6/14 MHz = 428.57 kHz for 6 MHz bandwidth. The thirteen segments may be combined in up to three hierarchical layers called Layer A, Layer B, and Layer C. Recently, a modified version of the ISDB-T modulation system called ISDB-T version B (ISDB-T_B) [2] was developed and adopted in Brazil and many other countries. The main difference of the ISDB-T_B modulation system is the RF channel and transmission mask [2], [3]. The ISDB-T_B modulation system can be divided into three stages composed of the re-multiplexor, the channel encoder, and the modulator as can be seen in Fig. 1. The ISDB-T_B modulator cannot be configured locally and depends on the multiplexer/re-multiplexer to control and configure all the processing stages. To illustrate the operation of these stages, this article presents a software simulation of the ISDB-T_B modulator.

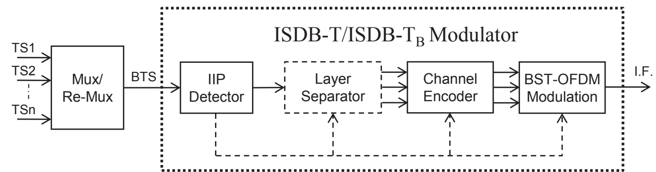

Fig. 1. Simplified diagram of the modulator.

From the Broadcast Transport Stream (BTS) that is generated in the multiplexing/re-multiplexing stage, all blocks that compose the modulator are described and analyzed using this computational tool. This simulator allows the monitoring of the input and output of all blocks in supported file formats with Matlab, C/C++ and support for Field Programmable Gate Array (FPGA). In addition, RF vectors can be created that can be transmitted by arbitrary signal generators. Fig. 2 shows a screenshot of this software, in which it is possible to select the file format, processing block, signal generator type and simulation time.

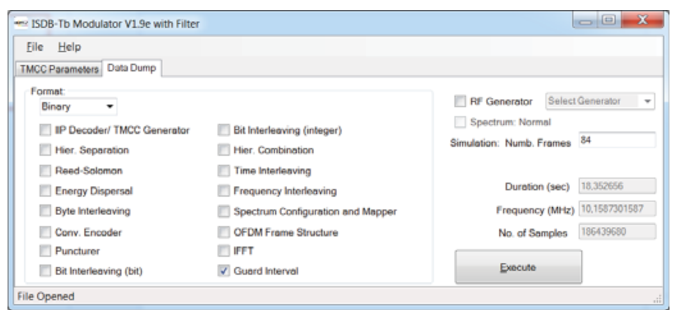

Fig. 2. Configuration screen of the ISDB-T_B simulator.

Thus, a review of the re-multiplexing stage is carried out in Section II. In Sections III and IV, the coding and modulation stages are presented. In Section V, the simulation tool is evaluated using an arbitrary signal generator and spectrum analyzer with an ISDB-T_B demodulator. Finally, in Section VI the conclusion is presented.

II. Re-multiplexing

To synchronize all the layers between the system source coding and modulation, the MPEG-2 TS 188 byte [4] from the source coding scheme, data carousel, etc. is multiplexed and re-multiplexed. The output of re-multiplexer is formed by a single TS with a size of 204 bytes and constant bit rate of four

This work was partly financed by FINEP and FOXCONN/MCT.
Cristiano Akamine is a Professor at the Engineering School of Mackenzie Presbyterian University, São Paulo, SP Brasil (e-mail: cristiano.akamine@mackenzie.br).
Yuzo Iano is a professor at UNICAMP in the Department of Communications for the Electrical Engineering and Computer Communications Faculty (DECOM / FEEC / UNICAMP), Campinas, SP, Brazil. (E-mail: yuzo@decom.fee.unicamp.br).

doi: 10.18580/setijbe.2015.3 Web Link: http://dx.doi.org/10.18580/setijbe.2015.3

© 2015 SET - Brazilian Society of Television Engineering / ISSN (Print): 2446-9246 / ISSN (Online): 2446-9432

times the sampling frequency of the Inverse Fast Fourier Transform (IFFT) modulator, or (4 x 512/63) = 32.5079Mb/s to 6 MHz bandwidth. Due to this characteristic the output signal of the re-multiplexer is called BTS [5]. The process of re-multiplexing is the positioning of each Transport Stream Packets (TSP) for each Layer and null TSP in a synchronized order with the demodulator of the receiver. The null TSP insertion maintains a constant BTS bit rate signal independent of the modulation parameters and channel coding. The packet order is required to secure the hierarchical transmission in a single TS and to minimize processing at the receiver [6].

The BTS signal is structured in a multiplexing frame in which the number of TSP depends on the mode and guard interval (GI) as can be seen in Table I [1], [2].

Additional the dummy byte, or 16 bytes in each BTS TSP is used to indicate the hierarchical layer that each TSP will be transmitted, TSP counter, frame headers, and the auxiliary data drivers, etc. Optionally, a Reed Solomon (RS) block code shortened (204,196,4) is applied and has correction capability of up to 4 bytes in a BTS TSP.

Fig. 3 shows an example of a TSP and multiplexer frame.

TABLE I
TSP NUMBERS INCLUDED IN A FRAME MULTIPLEXER

Mode	Guard interval reason			
	1/4	1/8	1/16	1/32
1 (2k)	1280	1152	1088	1056
2 (4k)	2560	2304	2176	2112
3 (8k)	5120	4608	4352	4224

The segment transmission order of the OFDM at the end of the modulation must be fully synchronized to the BTS signal frame multiplexer at the output of the re-multiplexer. Problems in the formation of the BTS signal multiplexer frame and clock and can generate a signal transmission error.

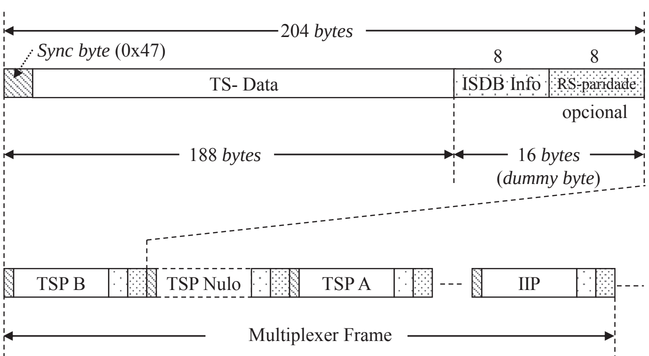

Fig. 3. BTS Frame Multiplexer.

Additionally the Modulation Configuration Control Information (MCCI) is sent in a package called ISDB-T Information Packets (IIP). The IIP is only transmitted once in the BTS signal multiplexer frame in which it has two descriptors that are called MCCI and Network Synchronization Information (NSI). The MCCI sets the modulation parameters and channel encoder as the size of IFFT, IG, modulation method, code rate, and the number of segments, etc. The NSI is used in the synchronization of the single frequency network in which the Synchronization Time Stamp (STS), maximum delay, control equipment, and product number, etc. are entered in this field.

Fig. 4 shows an example of an IIP for a BTS signal.

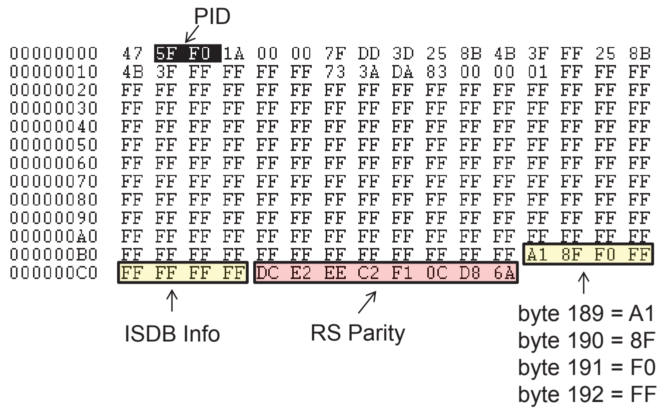

Fig. 4. IIP parameter identification.

III. ENCODER CHANNEL

The channel encoding process starts with IIP detection. The IIP can be identified by PID 0x1FF0 or by Layer 0x8 indication that can be obtained in the first four bits of byte 190. Reading descriptor IIP MCC, the TMCC generated is responsible for the configuration and control of all coding and modulation stages. In [1] and [2] it is possible to obtain the details of each bit for the MCCI and TMCC descriptors.

Fig. 5 shows the extracted IIP modulation parameters from Fig. 4 and Fig. 6 shows a simplified block diagram of the channel encoder. The detail of each of these blocks is presented in the following sub-sections.

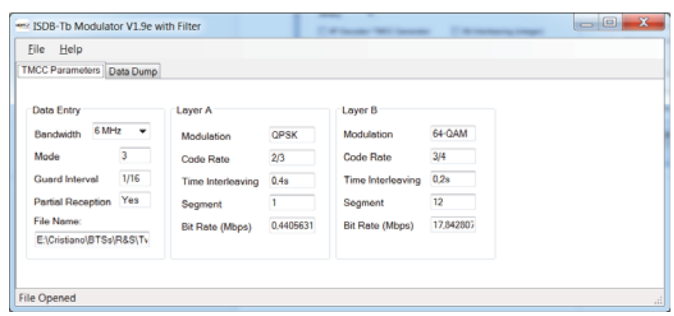

Fig. 5. Extracted IIP modulation parameters.

A. *Layer Separator*

The layer separator has the purpose of directing each BTS TSP to its respective layer. The separator reads BTS byte 190 and redirects each TSP according to the information contained in Table II. Null TSP and IIP are not transmitted in any of the hierarchical layers. The resulting output of the layer separator is an MPEG-2 TS, 188 bytes in size. Fig. 7 shows a Layer A TSP at the output of the separator.

© 2015 SET - Brazilian Society of Television Engineering / ISSN (Print): 2446-9246 / ISSN (Online): 2446-9432

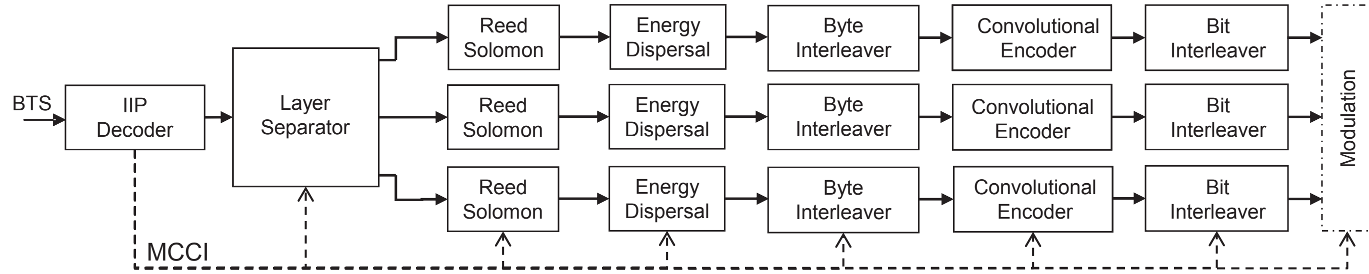

Fig. 6. Diagram of the channel coding stage.

TABLE II
ISDB FIELD LAYER INDICATOR INFO

byte 190 [7:4] (Layer Indicator)	Description
0000_b (0x0)	Null TSP
0001_b (0x1)	Layer A TSP
0010_b (0x2)	Layer B TSP
0011_b (0x3)	Layer C TSP
1000_b (0x8)	IIP TSP

```
00000000  47 01 01 20 B7 10 09 F5 D7 8C 00 FB FF FF FF FF
00000010  FF FF FF FF FF FF FF FF FF FF FF FF FF FF FF FF
00000020  FF FF FF FF FF FF FF FF FF FF FF FF FF FF FF FF
00000030  FF FF FF FF FF FF FF FF FF FF FF FF FF FF FF FF
00000040  FF FF FF FF FF FF FF FF FF FF FF FF FF FF FF FF
00000050  FF FF FF FF FF FF FF FF FF FF FF FF FF FF FF FF
00000060  FF FF FF FF FF FF FF FF FF FF FF FF FF FF FF FF
00000070  FF FF FF FF FF FF FF FF FF FF FF FF FF FF FF FF
00000080  FF FF FF FF FF FF FF FF FF FF FF FF FF FF FF FF
00000090  FF FF FF FF FF FF FF FF FF FF FF FF FF FF FF FF
000000A0  FF FF FF FF FF FF FF FF FF FF FF FF FF FF FF FF
000000B0  FF FF FF FF FF FF FF FF FF FF FF FF
```
Fig. 7. Layer A TSP.

B. Reed Solomon

The Reed Solomon (RS) block code was developed by two researchers, Irving S. Reed and Gustave Solomon in 1960 [7]. The RS code is considered a subclass of the Bose, Chaudhuri, and Hocquenghein (BCH) code for non-binary symbols [8]. The RS encoder is effective in correcting random errors and burst noise like the impulsive noise. The RS code is considered very powerful in relation to its error correction capability and is widely used in mobile communications; satellite; and storage devices such as CD, DVD; and bar codes.

ISDB-T uses an RS encoder (n=255, k=239, t=8), where n is the number of output symbols, k is the number of input symbols and t is the correction capability. Each symbol of this code uses m=8 bits. Due to this, MPEG-2 TS is standardized at 188 bytes, a modified version of this code called shortened RS is used with the following parameters RS(204,188,8). This version is obtained with the insertion and extraction of 51 null symbols at the beginning and end of the RS code.

The RS code uses algebra called Galois Field (GF) in which sum, subtraction, division, and multiplication are performed within this space. The GF(256) is generated from a field code generator $p(x)$ described in (1).

$$p(x) = x^0 + x^2 + x^3 + x^4 + x^8 \qquad (1)$$

Using (2) in GF(256) it is possible to calculate the polynomial generator g(x) in (3).

$$g(x) = (x + a^0)(x + a^1)(x + a^2) \dots (x + a^{2t-1}) \qquad (2)$$

$$g(x) = x^{16} + 59x^{15} + 13x^{14} + 104x^{13} + 189x^{12} + 68x^{11} + 209x^{10} + 30x^9 + 8x^8 + 163x^7 + 65x^6 + 41x^5 + 229x^4 + 98x^3 + 50x^2 + 36x^1 + 59 \qquad (3)$$

Considering the message to be coded $U(x)$, the encoded signal $V(x)$ can be obtained using (4) and (5) where $q(x)$ is the quotient and $r(x)$ is the remainder of the division.

$$\frac{U(x) \times x^{n-k}}{g(x)} = q(x) + \frac{r(x)}{g(x)} \qquad (4)$$

$$V(x) = U(x) \times x^{n-k} + r(x) \qquad (5)$$

Fig. 8 shows the TSP in Fig. 7 in the output of RS code. The addition of 16 bytes and the displacement of 1 byte can be seen. This displacement is necessary to maintain the synchronism with the OFDM frame.

```
00000000  01 01 20 B7 10 09 F5 D7 8C 00 FB FF FF FF FF FF
00000010  FF FF FF FF FF FF FF FF FF FF FF FF FF FF FF FF
00000020  FF FF FF FF FF FF FF FF FF FF FF FF FF FF FF FF
00000030  FF FF FF FF FF FF FF FF FF FF FF FF FF FF FF FF
00000040  FF FF FF FF FF FF FF FF FF FF FF FF FF FF FF FF
00000050  FF FF FF FF FF FF FF FF FF FF FF FF FF FF FF FF
00000060  FF FF FF FF FF FF FF FF FF FF FF FF FF FF FF FF
00000070  FF FF FF FF FF FF FF FF FF FF FF FF FF FF FF FF
00000080  FF FF FF FF FF FF FF FF FF FF FF FF FF FF FF FF
00000090  FF FF FF FF FF FF FF FF FF FF FF FF FF FF FF FF
000000A0  FF FF FF FF FF FF FF FF FF FF FF FF FF FF FF FF
000000B0  FF FF FF FF FF FF FF FF FF FF FF 6F 15 AD 7C 9
000000C0  BF F7 FF CD 5C 9D 71 D7 03 F4 43 47
```
Fig. 8. Layer A TSP output from the RS encoder.

C. Energy Dispersal

In one TS, there are many null packets or bytes with values 0xFF and 0x00 that are used to adjust the bit rate or compliment the number of bytes in a TSP. These packet sequences or bytes are often present at the source coding output and multiplexing.

To disperse these sequences, an interconnected energy dispersal at the RS output is used to reduce interference between symbols generated by the repetitive transmission of the same information.

This dispersal consists of a Pseudo Random Binary Sequence Generator (PRBS) and an adder module 2. The PRBS generator uses the polynomial generator $g(x) = 1 + x^{14} + x^{15}$. This generator consists of 15 shift registers and an adder module 2 that is connected to the output registers 14, 15

doi: 10.18580/setijbe.2015.3 Web Link: http://dx.doi.org/10.18580/setijbe.2015.3

and input register 1 as can be seen in Fig. 9. The sequence length of this generator is $2^{15} - 1 = 32767$, and is synchronized with the IIP and the TS clock of each layer. The disperser is initialized by a frame multiplexer with the word "100101010000000" and is disabled by a TSP synchronizing byte.

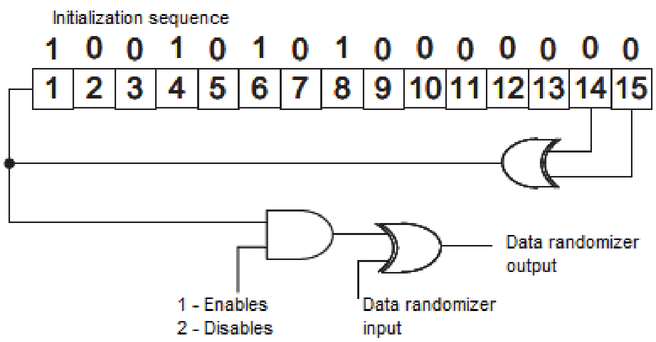

Fig. 9. Energy dispersal circuit.

Fig. 10 shows the TSP of Fig. 8 at the energy disperser output. It can be seen that the repetitive sequence of ones (0xFF) are dispersed.

```
00000000  02 F7 28 83 20 B1 56 44 45 68 4C 8C 4C D6 55 0
00000010  01 C3 FB 77 E4 CF A5 5E 20 3B 3F 65 7C A0 F4 3
00000020  C7 73 6C D4 95 04 81 E4 FB A5 E6 23 AB 36 05 4
00000030  E0 47 BE 6E 7A 9A E0 A1 BC 3A 77 62 CC B1 54 5
00000040  06 2F EB 1F 85 BE E2 79 B2 EA 51 82 1A F3 A1 D
00000050  3B 0B 65 C4 A3 64 34 A7 44 2C 67 16 AD 88 12 C
00000060  91 5E 98 38 AF 6C 1C 97 B4 8E 44 DA 65 22 A1 3
00000070  39 5F 68 3C 8F 74 DC C5 35 61 40 B8 7C 6E F6 9
00000080  C8 AB 4C 04 57 E6 0F AB DE 07 3B ED 67 90 AE 9
00000090  18 B7 AC 4E 16 5B 8A 26 C3 29 75 08 C1 CD 7B 5
000000A0  E4 1D A7 B2 2E 53 1A 15 A3 82 36 F3 49 D4 4B 0
000000B0  45 EA 63 82 B6 F0 49 DE 4B 3A 45 F2 8A E0 3F 3
000000C0  36 16 CB 8B E5 0A E4 A6 7C D3 41 47
```

Fig. 10. Layer A TSP at the energy disperser output

D. Byte interleaver

Interleavers are used in a wide variety of communication methods. An interleaver is a device that receives an alphabet of symbols and produces identical output symbols in a different order without increasing the bit rate. The interleaver disperses the bit sequences in order to minimize the block error effect in the middle of a data stream [9], [10].

These block errors are created from the impulsive noise of some equipment and selective fading in the communication channel. The error-correcting codes cannot correct errors that are concentrated in a sequence. Using interleavers, the sequence of symbols to be transmitted is scrambled and at the time that an accumulation of errors in the communication channel occurs, the decoder unscrambles the sequence spreading the errors. At that point, the error correcting codes can detect and correct errors.

The byte interleaver is a convolutional interleaver that uses time multiplexing and shift registers [11]. Each input multiplexer has a set of shift registers. The registers delay the bit sequence and then these bits are grouped again. In Fig. 11, it is possible to see how this interleaver is built. It has 12 branches *(B)* and 17-byte shift registers *(M)*. The *B* branches are cyclically connected to the energy disperser output and transfer 1 byte at a time via each branch. The first branch *(B_i=0)* has no memory, and the symbols are immediately transferred to the output. The byte interleaver aims to spread the packets from the Reed Solomon and the energy disperser to increase their efficiency before block errors occur.

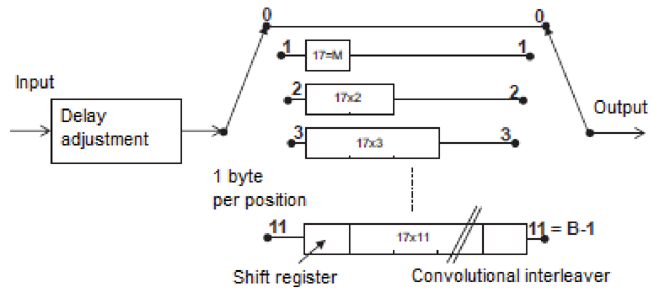

Fig. 11. Byte interleaver.

The maximum delay by the interleaver branch can be calculated by (6).

$$N = (B - 1) \times M \tag{6}$$

The delay generated by the convolutional interleaver can be calculated by (7) in which the equivalent of 2244 bytes is represented by 11 TSP consisting of 204 bytes each.

& L 0 H $ (7)

However, to keep all blocks synchronized with the frame multiplexer, a delay adjustment is inserted to supplement the number of TSP in a multiplexer frame. It is possible to calculate the number of TSP used in a multiplexer frame with the use of (8). This way, the synchronization delay value can be calculated using (9), where N_s is the number of segments, N_c is the number of data carriers, b_{QAM} is the number of bits per symbol in the primary modulation and R_{cc} is the rate of the convolutional encoder.

0 L ' H' H - H (8)

& L 0 F& (9)

Fig. 12 shows the packet in Fig. 10 at the byte interleaver output after 48 packets.

```
00000000  E5 23 85 76 78 3C A7 FC 6C 0D D0 8C 78 AD B2 E
00000010  1C 7A 76 C9 31 B3 1C 5E 5E 4C FC AF D0 8B F1 8
00000020  58 96 C8 D4 63 05 A3 87 E8 5A C0 6D 1E B3 76 4
00000030  7F 63 24 FC 70 05 1C 4D 83 79 2C 62 E9 D9 9E 3
00000040  1B 24 0E 1E E8 ED E7 79 B7 FF 41 39 FB 45 4A E
00000050  39 0B 80 C4 9C 6F B9 17 AF A9 36 98 7F B6 F5 C
00000060  31 3E 6C A0 66 6E 03 E9 94 6C 56 DA 60 21 7D 5
00000070  62 FF 93 DE 29 3A F5 C5 B9 D2 65 99 F6 B8 B3 B
00000080  48 11 14 04 6C AA AD 92 8D D6 FA 6A 50 C8 D4 9
00000090  C2 CC C4 94 E6 BD AD 79 C1 6D CD 08 A3 3F C4 3
000000A0  44 B4 06 D6 F1 B4 B5 15 38 6D 5A 08 39 23 D6 B
000000B0  26 78 D1 82 64 AA BC BB 94 AF 0C 36 CA 9C D1 3
000000C0  66 51 95 16 91 D1 CD 1B 12 E7 3C 47
```

Fig. 12. TSP output from the byte interleaver.

E. Convolutional Encoder

The convolutional codes were introduced by Elias in 1955 as an alternative to the use of block codes [12]. The substantial difference between block codes and convolutional codes lies

doi: 10.18580/setijbe.2015.3 Web Link: http://dx.doi.org/10.18580/setijbe.2015.3

in the fact that convolutional codes make use of memories, thus a given output at a certain time depends on not only some inputs at that very time, but also a time in the past *m*, where *m* is the number of memories [8]. A convolutional encoder (*n*, *k*, *m*) with *k* inputs, *n* outputs, and *m* memories may be implemented as a combinatorial sequential circuit which makes use of registers comprised of flip-flops, adder module 2 (or exclusive), and multiplexers/re-multiplexers. The rate of the convolutional encoder $R=k/n$ depends on the input *k* and the output *n*. Fig. 13 shows the combinational circuit used by ISDB-T$_B$ [1], [2].

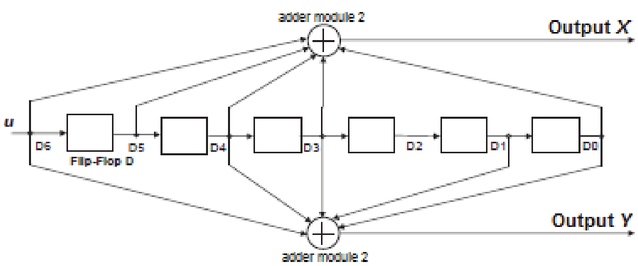

Fig. 13. Convolutional encoder (2,1,6) rate ½.

This convolutional code has mother rate R = 1/2, 64 states and its impulse response is expressed in (10).

$$g^{(0)} = 171_{oct}(1\,1\,1\,1\,0\,0\,1)$$
$$g^{(1)} = 133_{oct}(1\,0\,1\,1\,0\,1\,1) \quad (10)$$

Considering the input message u, X and Y outputs can be obtained using (11), where $\otimes$ represents the discrete convolution.

$$X = u \otimes g^{(0)}$$
$$Y = u \otimes g^{(1)} \quad (11)$$

Additionally, puncturing is used to discard some of the bits at the convolutional encoder output. This technique allows the bit rate to be varied, and the puncturing pattern can be seen in Table III. The P field indicates the bits that must be discarded and are represented by 0. The minimum free distance (dfree) of this convolutional code [13] is used as a performance parameter. In (12) it is possible to calculate the asymptotic gain of this code using a Viterbi decoder hard decision in relation to the uncoded modulation [14].

TABLE III
CONVOLUTIONAL ENCODER PUNCHING VALUES

Code rate (R)									
1/2		2/3		3/4		5/6		7/8	
P	d_{free}	P	d_{free}	P	d_{free}	P	d_{free}	P	d_{free}
X=1 Y=1	10	X=10 Y=11	6	X=101 Y=110	5	X=10101 Y=11010	4	X=1000101 Y=1111010	3

$$\delta = 10log_{10}\left(\frac{R \times d_{free}}{2}\right) \quad (12)$$

The bit interleaving is completed by a serial/parallel converter with variable size according to the modulation method. Thus, the input bits are converted from serial to parallel in dibit (2 bits), quadbit (four bits) or sixbit (6 bits) for the QPSK, 16-QAM, and 64-QAM modulations, respectively. The number of branches *B* of the interleaver is equal to the number of bits in each modulation method, and each branch has a specific delay. Because of these features, this interleaver is classified as a multiplexed convolutional interleaver [15]. The maximum branch delay is calculated using (13) and the total delay using (7).

$$N = \frac{120}{B-1} \quad (13)$$

TABLE IV
BIT INTERLEAVER DELAY ADJUSTMENT VALUE

Modulation	Mode 1(2k)	Mode 2 (4k)	Mode 3 (8k)
QPSK	uz ŧH 0 F tv r	yx ẑH 0 F tv r	s wu Hx0 F tv
16QAM	yx ẑH 0 F vz r	s wu Hx0 F vz	u ry Ht0 F vz
64QAM	s sw Ht0 F yt	t ur Hv0 F yt	v xr Hz0 F yt

To maintain the synchronism with the multiplexer frame, an additional delay is inserted, and its value can be obtained in Table IV where N_s represents the number of segments. Fig. 14 shows the bit interleaver diagram used in the 64-QAM modulation.

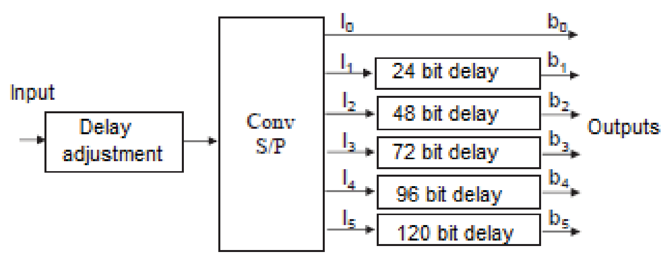

Fig. 14. Diagram of the bit interelaver used in the 64-QAM modulation.

IV. MODULATION

The ISDB-T$_B$ modulation stage can be seen in Fig. 15 and will be detailed in the following subsections.

A. Layer Combiner

The set of bits entering the layer combiner are grouped, and in this article are called symbols. It may be noted that our proposal is different from [1] and [2] and aims to reduce memory usage. Thus, the layer combiner performs the concatenation of the data symbols in all segments. For example, Mode 3 has 384 data carriers in each segment, this block groups all the segments amounting to 4992 symbols (carriers). Table V shows the distribution of the pilots in the three ISDB-T$_B$ modes.

doi: 10.18580/setijbe.2015.3 Web Link: http://dx.doi.org/10.18580/setijbe.2015.3

© 2015 SET - Brazilian Society of Television Engineering / ISSN (Print): 2446-9246 / ISSN (Online): 2446-9432

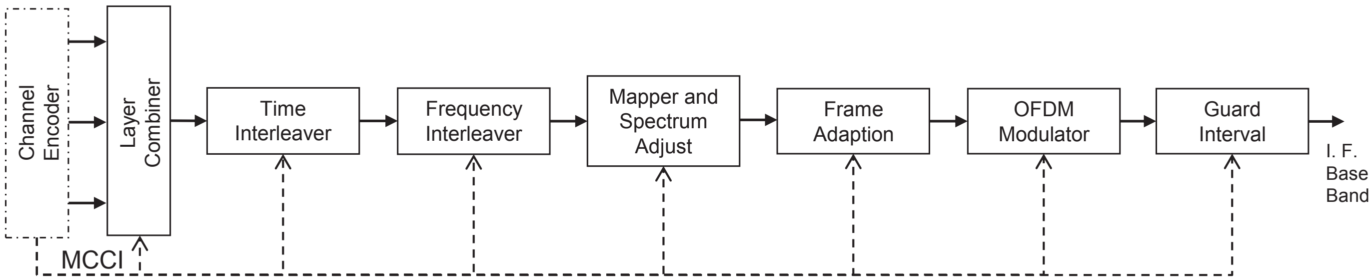

Fig. 15. Diagram of the modulation stage.

TABLE V
NUMBER OF CARRIERS USED IN THE COHERENT MODULATION

Carrier	Mode 1 (2k)	Mode 2 (4k)	Mode 3 (8k)
Total	108	216	432
Data (Nc)	96	192	384
SP	9	18	36
CP	0	0	0
TMCC	1	2	4
AC1	2	4	8
AC2	0	0	0

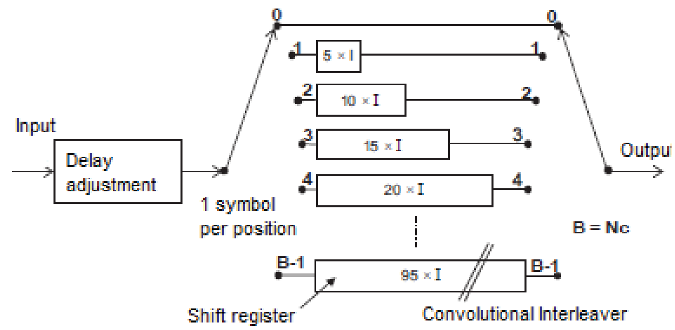

Fig. 16. Time interleaver.

B. Time Interleaver

After the layer combiner, the signal is interlaced. The time interleaver is formed by a convolutional interleaver that aims to interlace the carriers within various OFDM symbols. The time interleaver acts separately on each OFDM data segment and is cyclically combined at the output. The interleaving size can be adjusted by varying parameter *I*. In (14) it is possible to calculate the delay for each branch of the time interleaver, where *i* represents the number of each branch *i* = 0, 1, 2, ... *B* - 1 and mod is a function that returns the remainder of the division. The number of branches *B* of the time interleaver is equal to the number of data carriers.

$$D_i = mod(54 \times i, 96) \times 1 \qquad (14)$$

Table VI indicates the maximum time interleaver delay and the delay adjustment that is required to synchronize symbols within an OFDM frame. Fig. 16 shows a diagram of the interleaver and in Fig. 17 a scatter plot of the time intereaver of a segment in Mode 3. The time interleaver spreads the symbols from the modulation in each layer in which the length can be chosen, for the approximate values 0, 100, 200 and 400ms. The time interleaver increases the robustness of the system against impulsive noise and improves performance of mobile reception [16].

TABLE VI
TIME INTERLEAVER PARAMETERS IN MODE 3 (8K)

I	Maximum delay (symbols)	Delay adjustment (symbols)
0	0	0
1	95	109
2	190	14
4	380	28

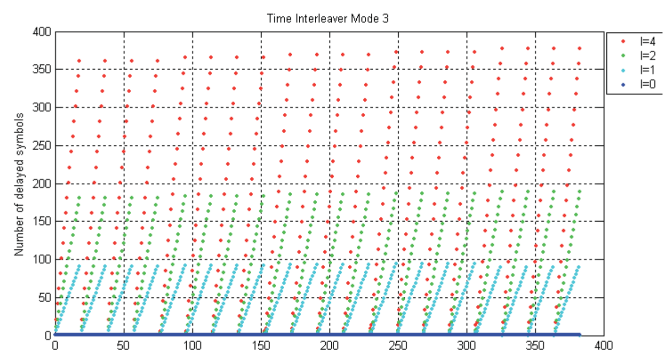

Fig. 17. Time interleaver scatter plot.

C. Frequency Interleaver

The frequency interleaver can be considered a block interleaver. In this interleaver symbols are written in a memory and read in a certain order. The frequency interleaver is performed in one OFDM symbol and is divided into three parts, as can be seen in Fig. 18.

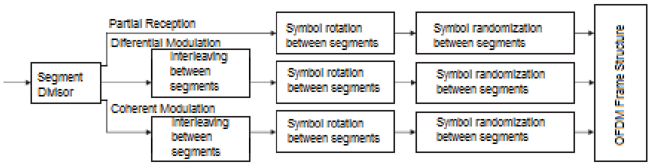

Fig. 18. Diagram of frequency interleaving.

The first type of interleaving performs carrier interleaving between the segments. If the partial reception option is enabled, the zero data segment is not scrambled. Fig. 19 shows the scatter plot of the interleaver used in the configuration shown in Fig. 5. It can be seen that symbols in the first segment enter and leave in the same order.

In Fig. 20, the carrier rotation within each segment can be seen. In Fig. 21, the carrier dispersion pattern within each segment can be seen. In [1] and [2] it is possible to obtain the tables and parameters of these interleavers. The final result, of frequency interleaving, can be seen in Fig. 22. Frequency interleaving is applied to the OFDM symbol that increases the system robustness against selective frequency fading [16]. Both the time interleaver and the frequency interleaver increase the error correction stage efficiency.

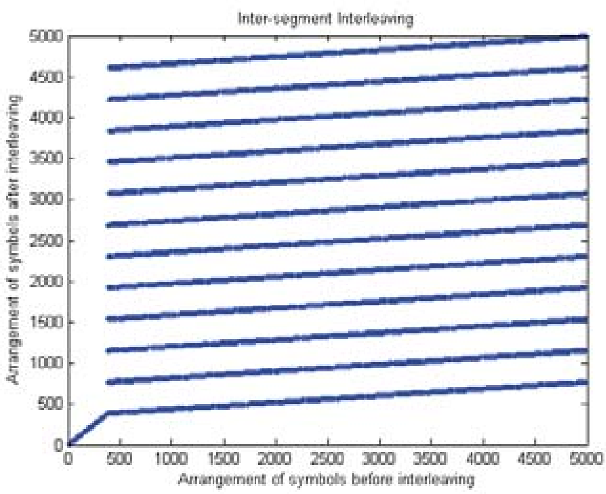

Fig. 19. Carrier dispersion interleaving between segments.

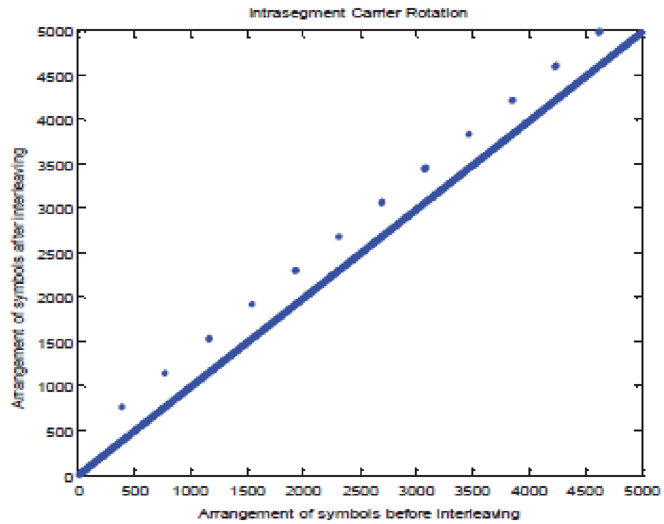

Fig. 20. Carrier rotation dispersion within each segment.

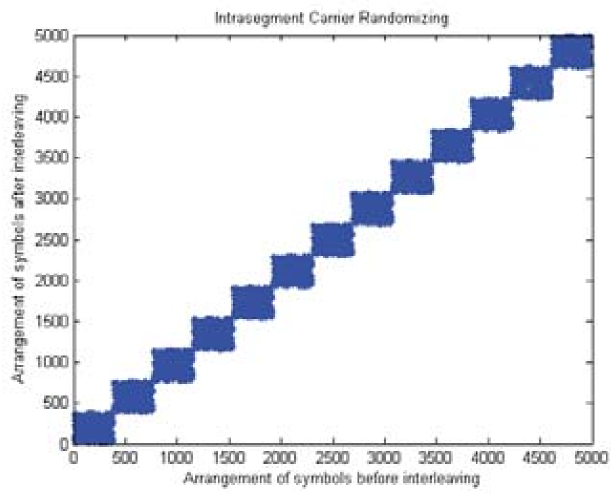

Fig. 21. Random interleaving dispersion between the segments.

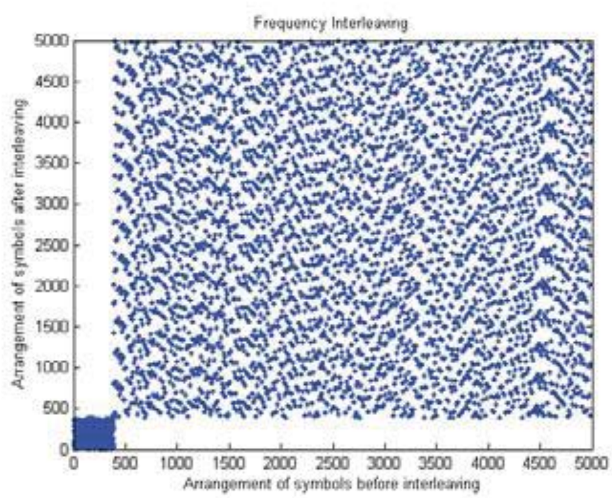

Fig. 22. Resulting dispersion from frequency interleaving.

D. Mapper and Spectrum Adjustment

After frequency interleaving, these symbols are modulated in QPSK, 16-QAM or 64-QAM through the use of a table.

Table VII shows the bit values, and the symbols for the QPSK modulation standardized to the power of 1 Watt. The tables for modulations 16-QAM and 64-QAM can be extracted from [1], [2].

TABLE VII
QPSK MODULATION VALUES

bit[1], bit[0]	In-phase	Quadrature
0.0	√‾t t	‾t t
0.1	‾t t	F‾t t
1.0	F‾t t	‾t t
1.1	F‾t t	F‾t t

Fig. 23 shows the constellations of the QPSK, 16-QAM, and 64-QAM modulations, respectively.

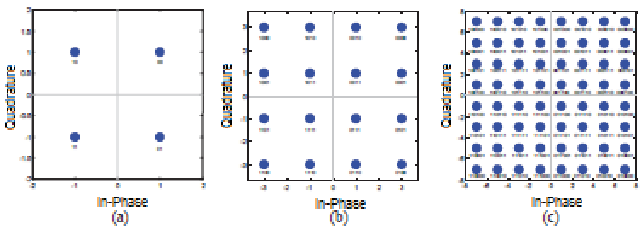

Fig. 23. ISDB-T system constellations: (a) QPSK (b) 16-QAM and (c) 64-QAM.

The spectrum adjustment is required to place the segments in the specific order established in [1] and [2]. Thus, the zero segment is positioned at the center of the spectrum and odd and even segments are distributed according to Fig. 24.

11	9	7	5	3	1	0	2	4	6	8	10	12

Fig. 24. Segment positions utilized after the spectrum adjustment.

E. *Frame Adaption*

The transmission signal is organized into frames. Each frame has a duration T_F and consists of 204 OFDM symbols. Each OFDM symbol has 13 segments and consists of a number of carriers, in Mode 1 K=1405 carriers (2k), K=2809 carriers in Mode 2 (4K), and K=5617 carriers in Mode 3 (8k) in which all are transmitted with the duration T_S. Fig. 25 shows an OFDM frame for a coherent modulation. Within the OFDM frame, Scattered Pilots (SP) and Continual Pilots (CP) are inserted and modulated in Binary Phase Shift Keying (BPSK) with a 33% power increase to guarantee the estimation and synchronization. The TMCC and Auxiliary Channel (AC) are inserted in the frame and modulated in Differential BPSK (DBPSK) with a 33% power increase for the purpose of signaling the modulation parameters, channel coding, frame synchronization, and transmission of auxiliary data. In total, 157 carriers out of 1405 carriers are used as pilots in Mode 1, 313 carriers out of 2809 carriers are used as pilots in Mode 2, and 625 carriers out of 5617 carriers are used as pilots in the Mode 3. In Fig. 26, the constellation of the frame adaption output can be seen. It can be seen that the SP pilots, TMCC, and AC are modulated in BPSK and possess greater potency than the QPSK and 64-QAM constellations.

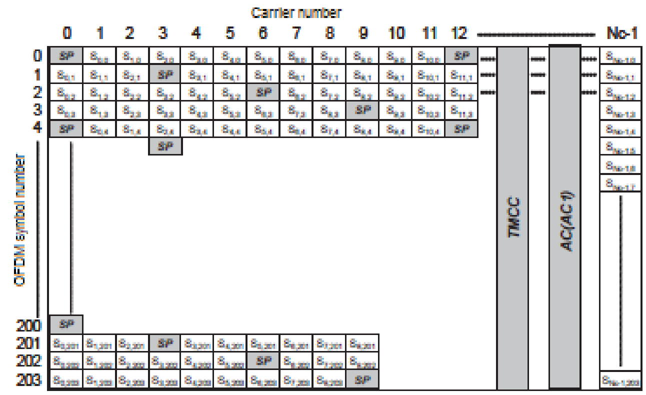

Fig. 25. OFDM frame structure for coherent modulation.

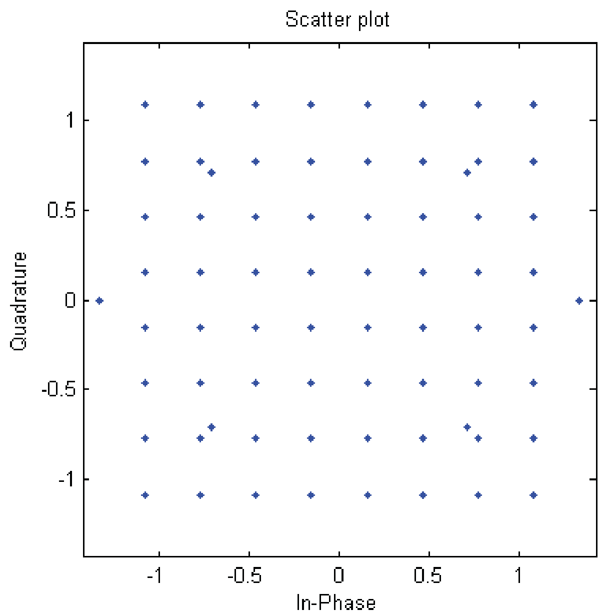

Fig. 26. Frame output adaptation constellation.

F. *OFDM Modulation*

The OFDM modulation appeared around the 1960s when Chang published his article on transmission synthesis with limited multi-channel bands [17]. He introduced the concept of transmitting messages across limited multiple channel bands without causing Inter-Carrier Interference (ICI) and Inter-Symbol Interference (ISI). In 1971, Weinstein and Ebert [18] used the Discrete Fourier Transform (DFT) to improve the performance of modulation and demodulation.

Due to the computational complexity of DFT and inverse DFT (IDFT), the Fast Fourier Transform algorithm (FFT) and Inverse Fast Fourier Transform (IFFT) discovered by Cooley and Tukey in 1965 [19] are used in modulation and demodulation, respectively. However, zeroes are added to the adapted frame output, to obtain the number of samples necessary to use IFFT and generate the useful part of the OFDM symbol (*Tu*). This technique is called zero padded

doi: 10.18580/setijbe.2015.3 Web Link: http://dx.doi.org/10.18580/setijbe.2015.3

[20], and the OFDM modulator block diagram can be seen in Fig. 27, where *Nc* represents the number. The IFFT size can be configured to one of three values, Mode 1 = 2k; Mode 2 = 4k; and Mode 3 = 8k.

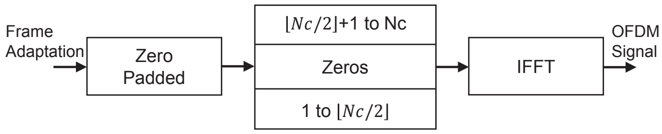

Fig. 27. OFDM modulator diagram.

G. *Guard Interval*

An important contribution to the OFDM modulation was made by Peled and Ruiz in 1980 [21], which introduced the cyclic prefix or cyclic extension, solving the orthogonality problem. Instead of using an empty guard space, they filled this space with a cyclic extension of the OFDM symbol.

The duration of the guard interval (Δ) is obtained by the duration $T_u \times k$, where k = 1/4; 1/8; 1/16; or 1/32. Thus, an OFDM symbol with duration T_s is composed of a guard interval with the duration Δ and T_u.

Fig. 28 shows an OFDM symbol with guard interval.

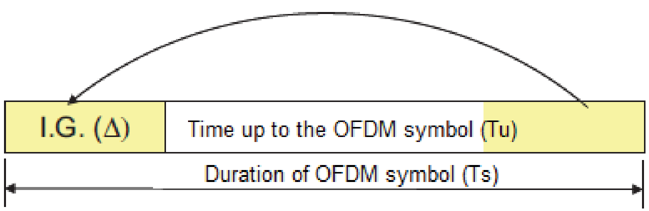

Fig. 28. Representation of the guard interval cyclic prefix.

In the BST-OFDM modulation, the common parameters for all layers are the IFFT size (Mode 1 = 2k, 4k Mode 2, and Mode = 3 = 8k) and the IG reason (1/4, 1/8, 1/16 and 1/32). The useful bandwidth used by ISDB-T is $6/14 \times 13$ corresponding to 5.57MHz.

In Fig. 29 the ISDB-T_B spectrum signal baseband in Matlab can be seen.

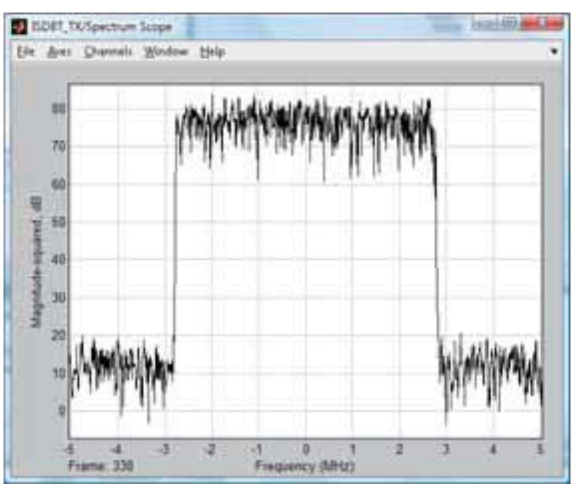

Fig. 29. ISDB-T_B spectrum baseband signal in Matlab.

V. Simulation Software

The simulator test was conducted with an arbitrary waveform generator and spectrum analyzer with an ISDB-T_B signal demodulation option. The RF vector from the simulator was installed in the generator and Bit Error Rate (BER), Modulation Error Rate (MER), and Mask Intermodulation tests were performed. Fig. 30 shows the equipment used in the tests.

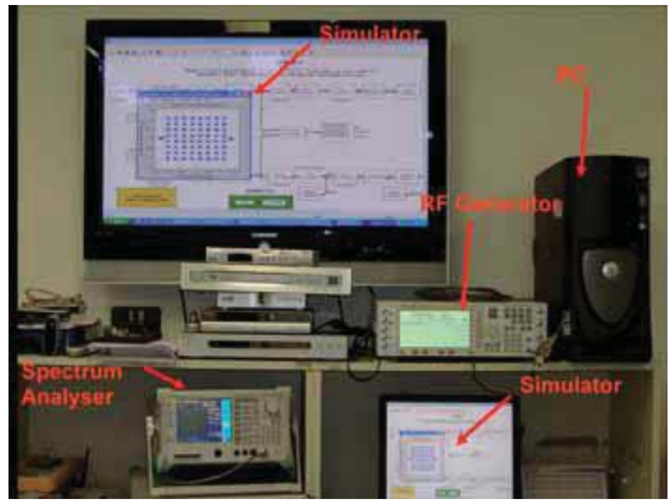

Fig. 30. Digital TV laboratory equipment used in the tests.

In the first test, it was verified that the ISDB-T_B signal generated by the simulator is within the mask transmission. Fig. 31 shows the result of this test.

In the Fig. 32, the measured bit error rate (BER) shows that the error is null before and after the RS in the two hierarchical layers. With this result, it can be concluded that all the stages of channel coding and simulated modulation function correctly. Furthermore, it can be seen that the modulation parameters detected through TMCC are the same as those in Fig. 5.

Figs. 33 and 34 show the MER measurement results. The value of MER is above 30 dB showing that any distortion in the modulation stage was introduced by the simulator.

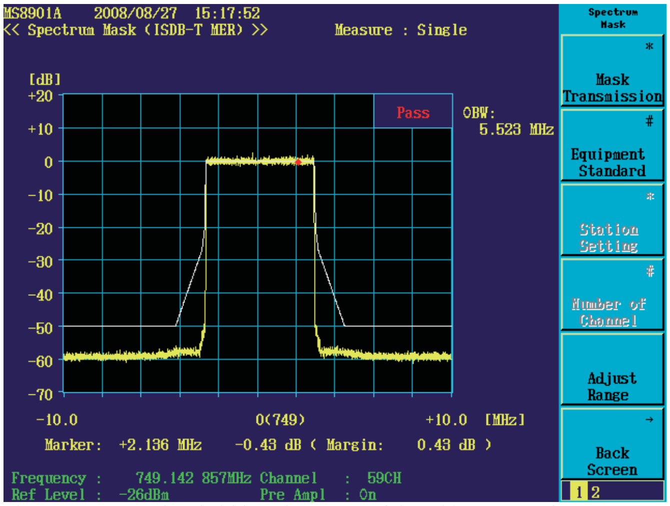

Fig. 31. Spectrum bandwidth at the output of the arbitrary waveform generator.

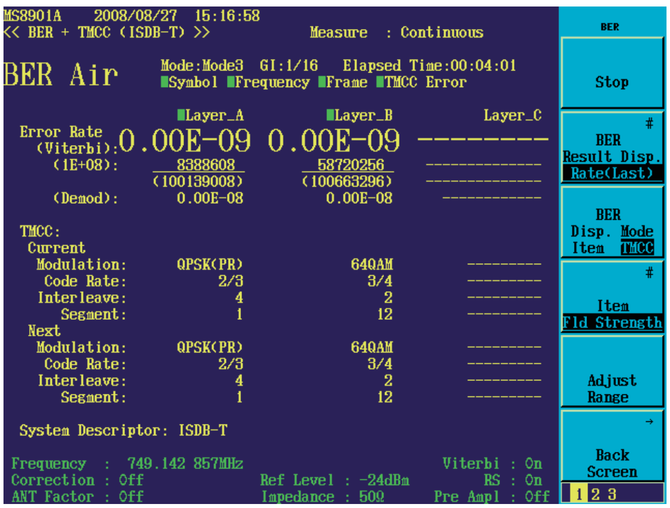

Fig. 32. Measurement of bit error rate before and after RS.

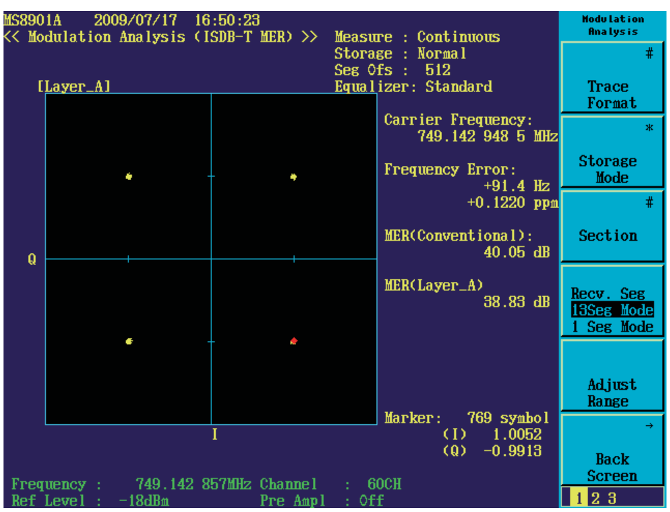

Fig. 33. MER measurements in Layer A.

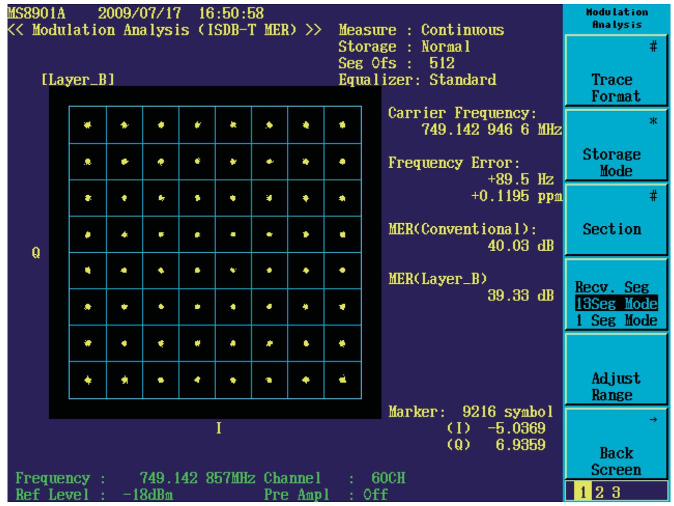

Fig. 34. MER measurements in Layer B.

VI. Conclusion

This paper presented a simulation tool that allows the analysis of all the blocks that make up an ISDB-T_B modulation to be completed. Numerical and graphical results were presented in order to illustrate the operation of an actual modulation system. Practical measures using an arbitrary waveform generator and spectrum analyzer were performed to demonstrate the compatibility of this simulation tool with the ISDB-T_B system.

Acknowledgment

The authors would like to thank RH-TVD CAPES and their colleagues at Mackenzie Digital TV Laboratory.

References

[1] *Transmission System for digital terrestrial broadcasting*, V1.6 E2 STD-B31, 2005.
[2] *Televisão digital terrestre – Sistema de transmissão*, ABNT NBR 15601:2007, 2007.
[3] G. Bedicks *et al.*, "Outlines of the Brazilian Digital Terrestrial Television Broadcasting System," presented at *57th annual IEEE Broadcasting Symposium*, Washington, DC, Oct. 1st–Nov. 2nd, 2007.
[4] *Generic coding of moving pictures and associated audio: Systems*, ISO/IEC 13818-1, Nov. 1994.
[5] C. Akamine *et al.*, "Re-multiplexing ISDB-T BTS into DVB TS for SFN," to be published in *IEEE Trans. Broadcasting* in December 2009.
[6] M. Uehara, "Application of MPEG-2 Systems to Terrestrial ISDB (ISDB-T)," *Proceedings of the IEEE*, vol. 94, no 1, 2006, pp. 261-268.
[7] I. S. Reed and G. Solomon, "Polynomial Codes over Certain Fields," *J. Soc. Ind. Appl. Math.*, vol. 8, pp. 300-304, 1960.
[8] S. LIN, D. Costello Jr, "*Error Control Coding: Fundamental and Applications"* 2nded. New York: Prentice Hall, 2004.
[9] SW. K. Andrews, C. Heegard, and D. Kozen, "A theory of interleavers," Department of Computer Science, Techical Report TR97-1634, June 1997.
[10] J. Ramsey, "Realization of optimum interleavers," *Information Theory, IEEE Transactions in*, vol.16, no.3, pp. 338-345, May 1970.
[11] G. D. Forney, "Burst-Correction Codes for the Classic Bursty Channel," *IEEE Transactions Communication. Technology.*, vol. COM-19, pp. 772-781, October 1971.
[12] P. Elias, "Coding for Noise Channels," *IRE Conv. Rec.,* Part 4, pp. 37-47, 1955.
[13] *Digital Video Broadcasting (DVB); Framing structure, channel coding and modulation for 11/12 GHz satellite services*, ETSI EN 300 421, 1997.
[14] S. Haykin, *Communication Systems,* 4th ed., New York: John Wiley & Sons, 2001.

[15] C. Heegard, and W. B. Stephen, *Turbo Coding*, Boston: Kluwer Academic Publishers, 1999.
[16] G. Bedicks *et al.*, "Results of the ISDB-T system tests, as part of digital TV study carried out in Brazil," *IEEE Trans. Broadcasting*, vol. 52, no.1, pp. 38–44, Mar. 2006.
[17] R. W. Chang, "Synthesis of band-limited orthogonal signals for multichannel data transmission," *Bell System Tech. J.*, vol. 45, pp. 1775-1796, Dec. 1966.
[18] S. B. Weinstein, and P. M. Ebert, "Data transmission by frequency division multiplexing using the discrete Fourier transform," *IEEE Trans.Commun*., vol. 5, pp. 628-634, Oct. 1971.
[19] J. Cooley and J. Tukey, "An Algorithm for the Machine Calculation of Complex Fourier Series," *Math. Comput.*, Vol. 10, no. 90, pp.297-301, Apr. 1965.
[20] R. V. Van Nee and R. Prasad, *OFDM for Wireless Multimedia Communications,* Norwood, MA: Artech House, 2000.
[21] A. Peled, and A. Ruiz, "Frequency domain data transmission using reduced computation complexity algorithms," in *Proc. IEEE Int. Conf.*Acoustic., Speech, Signal Processing, Denver, CO, 1980, pp. 964-967.

Cristiano Akamine received his B.Sc. degree in Electrical Engineering from Mackenzie Presbyterian University, São Paulo, Brazil, in 1999. He received his M.Sc. and Ph.D. degree in Electrical Engineering from the State University of Campinas (UNICAMP), São Paulo, Brazil, in 2004 and 2011 respectively. He is a professor of Embedded Systems, Software Defined Radio and Advanced Communication Systems at Mackenzie Presbyterian University. He is a researcher in the Digital TV Research Laboratory at Mackenzie Presbyterian University since 1998, where he has had the opportunity to work with many digital TV systems. His research interests are in system on chip for broadcast TV and Software Defined Radio.

Yuzo Iano graduated and obtained a doctorate at Universidade Estadual de Campinas (Unicamp) where he has acted as a professor since 1973. He is responsible for the Laboratório de Comunicações Visuais de Departamento Comunicações da Faculdade de Engenharia Eléctrica e de Computação de Unicamp (LCV/Decom/FEEC/Unicamp). His research covers telecommunications fields including digital signal processing, audio, video, and images.

Cite this article:
Akamine, C. and Iano, Y. ; 2015. Simulation Software for the ISDB-TB Modulation System. SET INTERNATIONAL JOURNAL OF BROADCAST ENGINEERING. ISSN Print: 2446-9246 ISSN Online: 2446-9432. doi: 10.18580/setijbe.2015.3 Web Link: http://dx.doi.org/10.18580/setijbe.2015.3